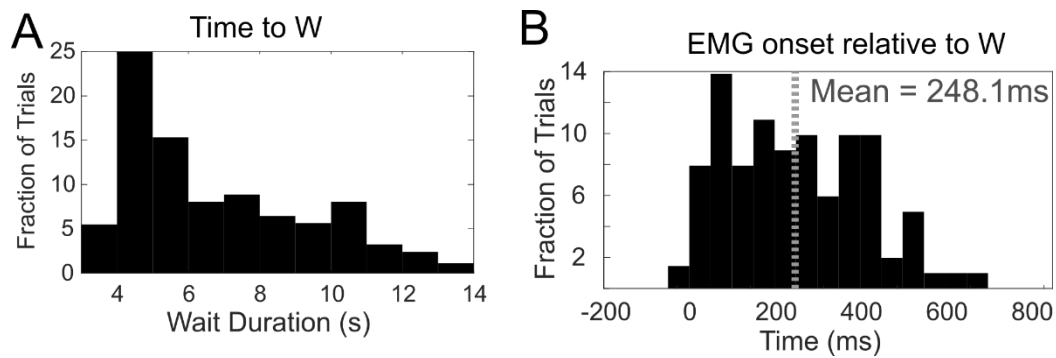
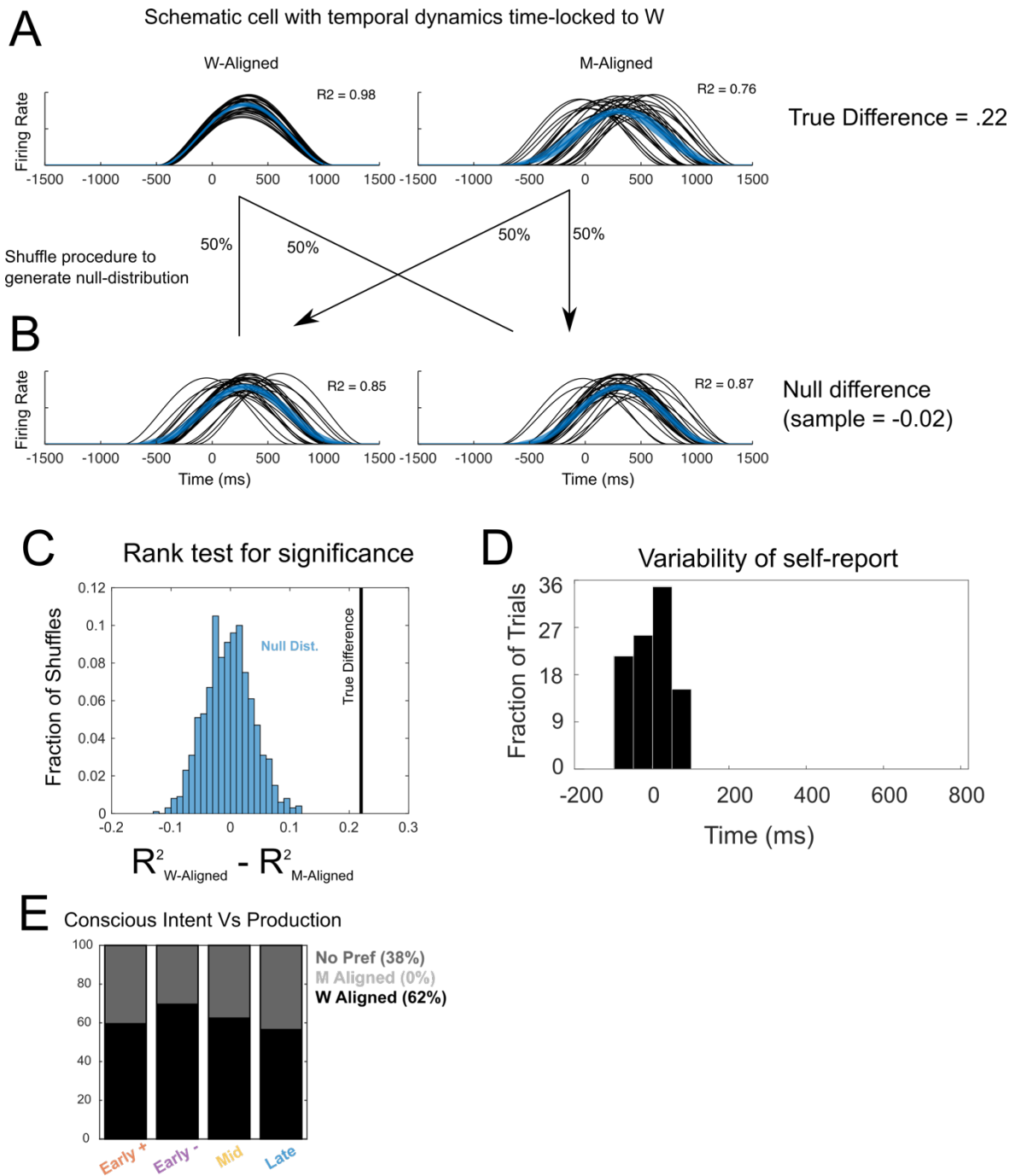


**Figure S1: Microelectrode array implantation locations. Related to Figure 1.** Individual participant anatomy with the location of microelectrode array implants. Implantation sites correspond to anterior portions of the PPC superior to the intraparietal sulcus.



**Figure S2. Summary of behavior during the first experiment, Related to Figure 1.** **A)** Distribution of intervals between the cue informing which of two possible actions to perform and the time the subject first reported the urge to initiate movement. **B)** Trial-to-trial variability between the time the subject reports the urge to initiate action and the time of EMG onset. Due to paralysis below shoulder level, figure data is restricted to shoulder shrug trials as these movements enabled EMG recording.



**Figure S3. Neural signals better correlate to the timing of motor production (EMG onset, “M”) than the experienced urge to initiate movement (“W”), Related to Figure 1.** Here we schematically illustrate the process of determining whether neural timing better correlates with M or W. The underlying logic rests on the significant variability in the timing between M and W, which allows us to ask whether neural timing better aligns to M or W. **A)** Schematic of approach illustrating the effect of misaligning a neuron to M if the signals are time-locked to W. The difference in explained variance quantifies how well the two distinct alignment points account for trial-to-trial variability of the neural responses. **B)** To measure the significance of the difference in explained variance, a null distribution of differences was

generated by randomly assigning W-aligned and M-aligned trials to two distributions for comparison. **C)** Comparison of true difference to null distribution and rank-test. **D)** A major complication interpreting our analysis is that M and W likely have different associated measurement errors. EMG recordings have high signal-to-noise providing precise estimates of onset (<50 ms error). Quantifying the measurement error of the subject's self-report is challenging; however, we can estimate the variability intrinsic to our subjects reporting the timing of events using the clock dial. To do this, we played an audible beep and asked the subject to report the beep's time based on the clock dial's position. Panel A shows the associated measurement error between the true position of the clock dial when an auditory cue was presented and the subject's report of the position (converted to ms). For comparison, the distribution is presented in the same range as Figure S2B. The measurement variance when reporting the beep time was significantly reduced compared to the variance between the time of the subjective report and motor awareness (Two-sample F-test,  $p < 0.05$ ). This suggests that while there is some inherent noise in using the clock's position to report the timing of events, a sizeable portion of the trial-to-trial variability between M and W reflects true trial-to-trial variability between movement onset and the experienced urge to move. **E)** Does the measurement variability introduced by the clock paradigm make it impossible to identify neurons time-locked to W? We approached this question with the following simulation. First, neural time courses were aligned to minimize temporal trial-to-trial variability. These aligned units were then temporally shifted by amounts drawn from our estimate of measurement error (Panel D). This dataset represents the expected neural recordings if neurons are time-locked to W, and the source of trial-to-trial temporal variability is measurement noise introduced by the clock paradigm. The registered neural signals were also realigned by amounts drawn from the trial-to-trial estimates of the difference between M and W (Figure S2B.) This dataset represents the effect of misaligning W-aligned data to M. We then analyzed the resulting data as illustrated in Figure S3A-C. Given the measurement noise associated with the clock paradigm and the sensitivity of our analysis procedure, can we correctly identify that the simulated data is aligned to W? This analysis was done separately for each unit, and the results are reported categorized by the clusters reported in Figure 1D. As shown in this panel, given the assumption that the measurement noise inherent in the clock paradigm is well captured by the sensory test, we should be able to identify W-aligned units if they existed in our recorded neural population.

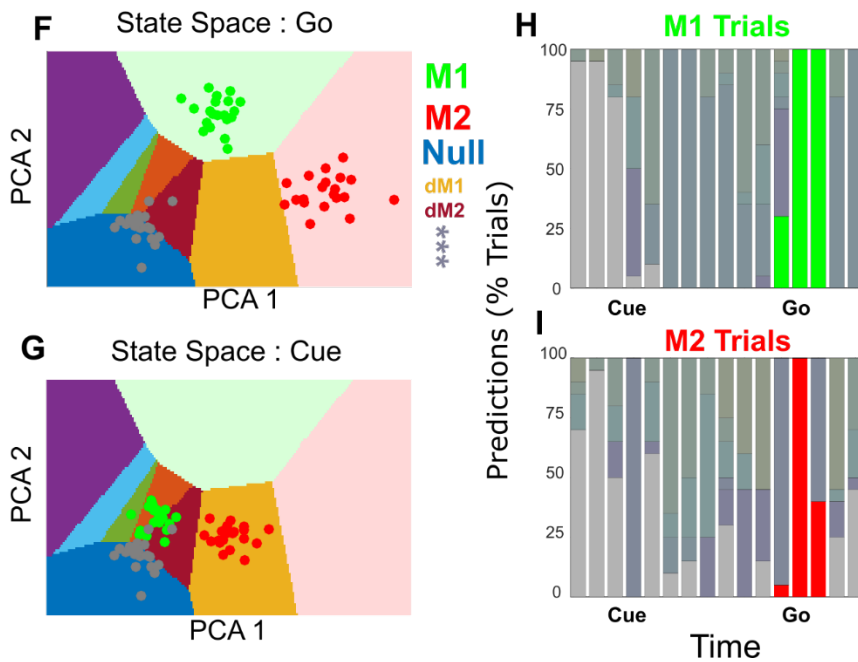
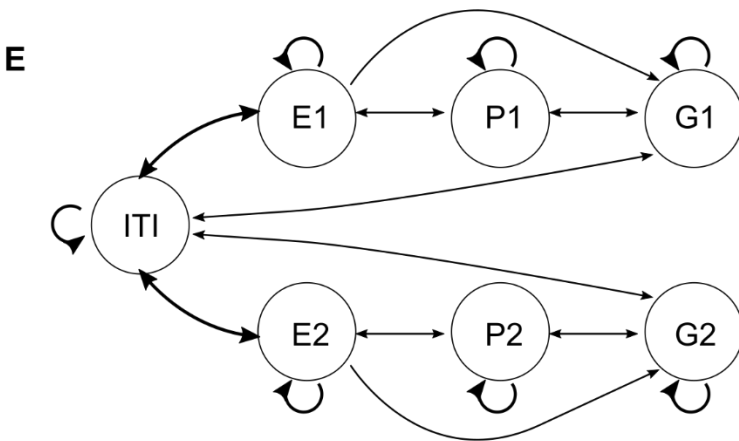
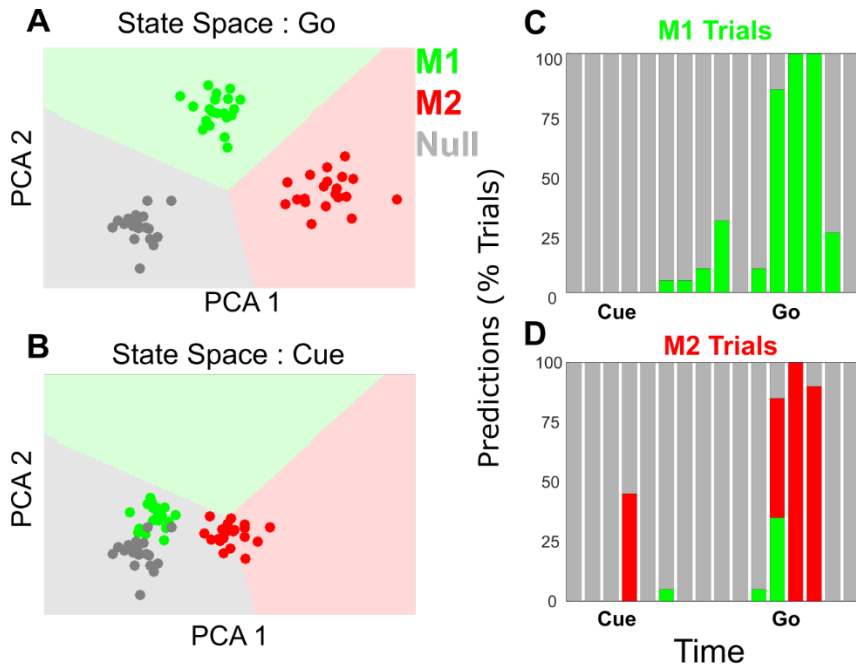


**Figure S4. Improved algorithms and parameterization ensure neural decoding aligns with participant choice, Related to Figure 4.** A-D) Simple classification methods fail to uniquely identify the intention to initiate movement. **A)** Neural data and decision boundaries in the first two principal components. Points represent single-trial activity recorded during the ITI (grey) and Go epochs (Movement 1/M1 = green and Movement 2/M2 = red; 250-750 ms after reported urge to move). The background shows the division of PCA space into class affiliated regions as determined by LDA applied to the plotted trial activity. **B)** Similar to A, except trial projections are taken from a time window just following the cue (250-750 ms). C-D) Spurious early intention decoding: Classifier trained on Go epoch neural data (Panel A) is applied throughout the trial interval. Each bar shows the classifier prediction on held-out data (movement 1, movement 2, or null) for each slice of time (500ms non-overlapping windows as in Figure 3). **C)** Result when applied to M1 trials. **D)** Result when applied to M2 trials. **E)** State transition model used for Hidden Markov Model decoding of two possible movements. Nodes (circles) denote states. Edges (arrows) denote state transitions. ITI = inter-trial interval (-1500 to -1000 ms pre-cue.) Ex = Early plan (250 to 750 ms post-cue.) Px = Late plan (-1500 to -1000 ms pre-W.) Gx = Go (250 to 750 ms post-W.) **F-I)** Improving continuous classification. **F-G)** Similar to A, B, however, now with additional state definitions. **H-I)** Similar to C, D, however, now with additional state definitions and HMM decoding.